The Arabidopsis GAGA-Binding Factor BASIC PENTACYSTEINE6 Recruits the POLYCOMB-REPRESSIVE COMPLEX1 Component LIKE HETEROCHROMATIN PROTEIN1 to GAGA DNA Motifs[1]

Andreas Hecker, Luise H. Brand, Sébastien Peter, Nathalie Simoncello, Joachim Kilian, Klaus Harter, Valérie Gaudin, and Dierk Wanke*

Center for Plant Molecular Biology, Plant Physiology, and Biophysical Chemistry, University of Tübingen, 72076 Tuebingen, Germany (A.H., L.H.B., S.P., J.K., K.H., D.W.); Institut National de la Recherche Agronomique, Unité Mixte de Recherche 1318 AgroParisTech, Institut J.-P. Bourgin, Institut National de la Recherche Agronomique Centre de Versailles-Grignon, F–78026 Versailles, France (N.S., V.G.); and Universität des Saarlandes, Molekulare Pflanzenbiologie, 66123 Saarbruecken, Germany (D.W.)

ORCID IDs: 0000-0002-2150-6970 (K.H.); 0000-0002-7083-1550 (D.W.).

Polycomb-repressive complexes (PRCs) play key roles in development by repressing a large number of genes involved in various functions. Much, however, remains to be discovered about PRC-silencing mechanisms as well as their targeting to specific genomic regions. Besides other mechanisms, GAGA-binding factors in animals can guide PRC members in a sequence-specific manner to Polycomb-responsive DNA elements. Here, we show that the Arabidopsis (*Arabidopsis thaliana*) GAGA-motif binding factor protein BASIC PENTACYSTEINE6 (BPC6) interacts with LIKE HETEROCHROMATIN PROTEIN1 (LHP1), a PRC1 component, and associates with VERNALIZATION2 (VRN2), a PRC2 component, in vivo. By using a modified DNA-protein interaction enzyme-linked immunosorbant assay, we could show that BPC6 was required and sufficient to recruit LHP1 to GAGA motif-containing DNA probes in vitro. We also found that LHP1 interacts with VRN2 and, therefore, can function as a possible scaffold between BPC6 and VRN2. The *lhp1-4 bpc4 bpc6* triple mutant displayed a pleiotropic phenotype, extreme dwarfism and early flowering, which disclosed synergistic functions of LHP1 and group II plant BPC members. Transcriptome analyses supported this synergy and suggested a possible function in the concerted repression of homeotic genes, probably through histone H3 lysine-27 trimethylation. Hence, our findings suggest striking similarities between animal and plant GAGA-binding factors in the recruitment of PRC1 and PRC2 components to Polycomb-responsive DNA element-like GAGA motifs, which must have evolved through convergent evolution.

Transcription factors (TFs) control expression by specific binding to cis-regulatory DNA elements close to a gene and, thereby, modulating the activity of the transcription machinery (Badis et al., 2009; Rohs et al., 2009). For the majority of these regulatory proteins, it is not well understood how they act at the molecular level to govern gene expression tightly, in a spatial and temporal manner, and to orchestrate diverse cellular processes such as development or the plasticity to respond to environmental stimuli. Some TFs affect polymerase activity directly, while others function as recruitment factors or as modifiers that change the accessibility of cis-regulatory DNA elements through posttranslational modifications of histones (Cedar and Bergman, 2009; O'Meara and Simon, 2012).

GAGA-motif binding factors (GAFs) are polyvalent TFs that appear to act through diverse molecular mechanisms in the control of homeotic gene expression during development (Lehmann, 2004; Adkins et al., 2006). There are two unrelated GAF families in animals, Trithorax-like (Trl) and Pipsqueak (Psq), which compete for the same GAGA-motif containing DNA sequences and are involved in similar regulatory processes (Lehmann, 2004; Adkins et al., 2006; Kasinathan et al., 2014). Both GAF families play key roles in the context-dependent regulation of gene expression by communicating with histone-modifying complexes

(Huang et al., 2002; Schuettengruber and Cavalli, 2009; Wang et al., 2010; Li et al., 2013). Psq is essential for silencing homeotic genes through sequence-specific targeting of POLYCOMB-REPRESSIVE COMPLEX2 (PRC2) members to certain genomic loci, which are involved in the deposition of a repressive trimethylation mark at Lys-27 in histone H3 (H3K27me3; Huang et al., 2002; Schuettengruber and Cavalli, 2013). Similarly, the Trl GAF mediates a sequence-specific recruitment of different PRC1 members to GAGA motif-containing Polycomb-responsive DNA elements (PREs; Faucheux et al., 2003; Mishra et al., 2003; Mulholland et al., 2003; Salvaing et al., 2003; Schwartz and Pirrotta, 2008). Although the existence of plant PRE-like elements has been proposed (Santi et al., 2003; Schatlowski et al., 2008; Buzas et al., 2012), no PRE-like element or GAF homologs have been identified in plants so far.

Members of the plant-specific BARLEY B RECOMBINANT (BBR)/BASIC PENTACYSTEINE (BPC) family have GAGA motif-binding properties and are involved in the control of homeotic genes (Sangwan and O'Brian, 2002; Santi et al., 2003; Kooiker et al., 2005; Brand et al., 2010; Berger et al., 2011; Simonini and Kater, 2014). Phylogenetic analysis disclosed three groups of plant BBR/BPC proteins and a high degree of conservation within these groups that is indicative of a strong positive selection throughout evolution (Meister et al., 2004; Lang et al., 2010; Wanke et al., 2011). All BBR/BPC proteins possess the highly conserved BPC DNA-binding domain at their C terminus but differ by domains in the N terminus (Meister et al., 2004; Wanke et al., 2011). Similar to animal GAFs, group I BBR/BPC proteins control the expression of homeotic genes during developmental processes, while a molecular function for group II and III BBR/BPC proteins remains elusive (Wanke et al., 2011). Barley group I BBR is involved in leaf and flower development by regulating the expression of *Barley Knotted3 (BKn3)*, the ortholog of the homeobox gene *Knotted1 (Kn1)* from maize (*Zea mays*; Santi et al., 2003). An intragenic duplication of a GAGA motif in the *Bkn3* gene contributes to the dominant *hooded* mutation, where the BBR-dependent ectopic overexpression of *BKn3* in the flower meristem abolishes seed development (Santi et al., 2003). Accordingly, group I BBR/BPC proteins regulate *SHOOTMERISTEMLESS* and *BREVIPEDICELLUS* in Arabidopsis (*Arabidopsis thaliana*), which are orthologs of barley (*Hordeum vulgare*) *BKn3* or maize *Kn1* (Simonini and Kater, 2014). The group I BBR/BPC protein BPC1 is essential for the activation of the TF genes *LEAFY COTYLEDON2 (LEC2), INNER NO OUTER (INO),* and *SEEDSTICK (STK),* which control ovule and embryo development (Meister et al., 2004; Kooiker et al., 2005; Berger et al., 2011). Moreover, group I BBR/BPC members have the capacity to bend DNA, presumably through a molecular mechanism that involves multimerization of the proteins (Kooiker et al., 2005; Simonini et al., 2012). In addition, Arabidopsis BPC1 regulates MADS box gene expression and the recruitment of the SEUSS

(SEU)-LEUNIG (LUG) transcriptional suppressor complex to repress the homeotic *STK* locus (Simonini et al., 2012). These findings on plant GAFs are reminiscent of the tight control of homeotic genes described for animal GAF families.

Here, we show that Arabidopsis BPC6, a group II BBR/BPC protein, interacts with the core PRC1 component LIKE HETEROCHROMATIN PROTEIN1 (LHP1) both in vitro and in vivo. Our data suggest the existence of a group II BPC-dependent protein complex in the nucleoplasm that contains LHP1 and that may also comprise the plant PRC2 member VERNALIZATION2 (VRN2). Furthermore, we show that BPC6 is required and sufficient for the recruitment of LHP1 to GAGA motifs in vitro. Consistently, GAGA motifs in promoters coincide with in vivo LHP1 target genes and H3K27me3 decoration. The *lhp1-4 bpc4 bpc6* triple mutant displays pleiotropic developmental defects that suggested a synergistic interaction between LHP1 and group II BPCs. This synergy was supported by transcriptome analyses, where differentially expressed (DE) genes in the triple mutant were enriched for TF genes and known H3K27me3 targets. Our data indicate a molecular role for group II BBR/BPC proteins in the recruitment of Polycomb components to GAGA motifs in plants, which emphasizes evolutionary similarities between animal and plant GAF function.

RESULTS

BPC6 Interacts with LHP1 and Colocalizes with PRC2 Components in Vivo

The Arabidopsis BBR/BPC family consists of seven members that are divided into three groups. Group II consists of *BPC4* and *BPC6* as well as *BPC5*, which is a putative pseudogene (Meister et al., 2004; Monfared et al., 2011). We tested the possible physical interaction of BPC6 with selected plant Polycomb Group (PcG) components and chromatin-remodeling factors by yeast (*Saccharomyces cerevisiae*) two-hybrid analysis (Fig. 1). The previously described formation of BPC6 homodimers served as a positive control (Wanke et al., 2011). Only the PRC1 component LHP1 disclosed a positive interaction with BPC6 in yeast (Fig. 1A), whereas no physical interaction was observed between BPC6 and any other tested protein, such as SWINGER (SWN), FASCIATA2 (FAS2), FERTILIZATION-INDEPENDENT ENDOSPERM (FIE), MULTICOPY SUPPRESSOR OF IRA1 (MSI1), or VRN2. To confirm our findings, we studied the interaction between BPC6, LHP1, and control proteins in transiently transformed *Nicotiana benthamiana* cells by noninvasive in vivo fluorescence lifetime measurement (FLIM), where fluorescent fusion proteins localize freely to their endogenous nuclear domains (Supplemental Fig. S1). As no physical interaction between donor (e.g. GFP) and acceptor (e.g. red fluorescent protein [RFP]) chromophores exists, a significant GFP-donor lifetime decrease is an explicit indication for

Figure 1. BPC6 interacts with the PRC1 component LHP1 in vivo and tightly associates with the PRC2 core component VRN2. A, Yeast two-hybrid analyses revealed positive interaction between BPC6 and LHP1. No interaction was found with SWN, FAS2, FIE, MSI1, and VRN2. AD, Activation domain; BD, DNA-binding domain; CSM-LW, complete supplement mixture without Leu and Trp; CSM-LWH, complete supplement mixture without Leu, Trp, and His. B, Noninvasive FLIM of BPC6-GFP or BPC1ΔDBD-GFP in the presence of LHP1-RFP, RFP-LHP1, VRN2-RFP, and RFP-VRN2 in transiently transformed *N. benthamiana* epidermis cells. Significant GFP-lifetime decrease was detected for BPC6 with LHP1 and VRN2, which indicates the close proximity of these proteins in vivo ($P < 0.05$). Group I BPC1ΔDBD-GFP exhibited no significant GFP-lifetime decrease with LHP-RFP. Error bars indicate sd ($n \geq 6$). C, BiFC assay in transiently transformed *N. benthamiana* epidermis cells. BPC6/LHP1 and LHP1/VRN2 heterodimers were formed predominantly in the nucleoplasm. The formation of BPC6 homodimers served as a positive control in all experiments. Bars = 10 μm.
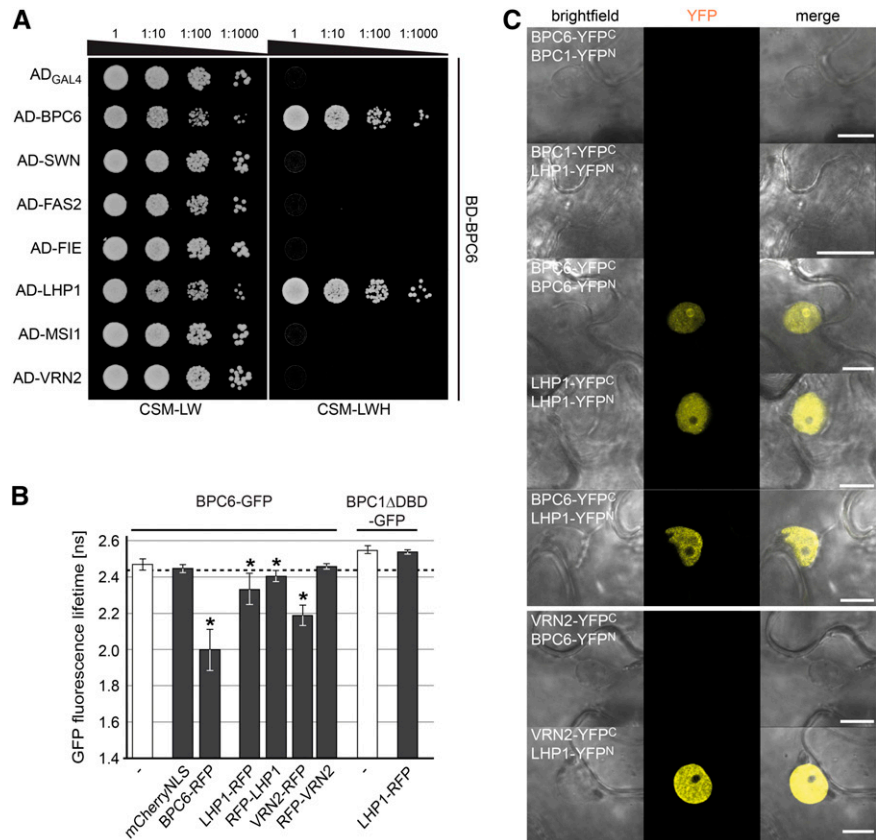
the very close proximity of donor and acceptor fusion proteins in vivo that is probably caused by direct physical interaction (Elgass et al., 2010; Wanke et al., 2011; Harter et al., 2012). In full agreement with our yeast two-hybrid data, a significant BPC6-GFP lifetime decrease was detectable when coexpressed with BPC6-RFP, LHP1-RFP, or RFP-LHP1 but also with VRN2-RFP as an acceptor chromophore (Fig. 1B). In contrast, no decrease in GFP-donor lifetime was detected when the group I BBR/BPC protein fragment BPC1ΔDBD-GFP was used as donor or RFP-VRN2 and mCherry-NLS (for nuclear localization signal) fusion proteins were used as possible acceptors (Fig. 1B). It is noteworthy that LHP1 and VRN2 lifetime decreases were orientation dependent and strongest with C-terminal RFP fusions. However, both orientations resulted in significant lifetime decreases for LHP1 and BPC6, which confirmed our yeast two-hybrid results in planta. In addition to FLIM, we confirmed our findings by noninvasive Förster resonance energy transfer between the BPC6-GFP donor and different RFP fusion acceptor chromophores in individual *N. benthamiana* nuclei (Supplemental Fig. S2).

LHP1 Interacts with BPC6 and VRN2 in the Nucleoplasm

To identify in which subnuclear domain the interaction between BPC6 and LHP1 takes place, we used bimolecular fluorescence complementation (BiFC) experiments.

BPC6/LHP1 heterodimers formed predominantly in the nucleoplasm (Fig. 1C) but not in the nucleolus or other subdomains where BPC6-GFP is localized (Supplemental Fig. S1; Wanke et al., 2011). This localization reflected the known distribution of LHP1 (Libault et al., 2005), which indicated the existence of at least two distinct pools of BPC6, one that interacts with LHP1 in the nucleoplasm and a second that localizes to the nucleolus and fulfills other, yet unknown functions. Interestingly, BPC4, the group II paralog of BPC6 (Monfared et al., 2011; Wanke et al., 2011), was also able to interact with LHP1 in BiFC assays (Supplemental Fig. S3).

Our data revealed no physical interaction but a close proximity of BPC6 with the PRC2 component VRN2, which suggested that LHP1 might function as a scaffold and link PRC1 and PRC2 function. Hence, a significant lifetime decrease between Arabidopsis BPC6 and VRN2 in the heterologous *N. benthamiana* system (Fig. 1B) is possibly mediated by endogenous tobacco (*Nicotiana tabacum*) LHP1 orthologs as scaffolds. By BiFC experiments, we could show that VRN2 was also able to interact directly with LHP1 (Fig. 1C). Thus, the lifetime reduction of BPC6-GFP coexpressed with VRN2-RFP in our FLIM experiment (Fig. 1B) can readily be explained by the close proximity of BPC6 with VRN2, because all proteins interacted in vivo with LHP1, possibly in a higher order complex. A similar scaffolding function of LHP1 for PRC1 and

PRC2 was also reported for the interaction between LHP1 and MSI1 (Derkacheva et al., 2013).

BPC6 Interacts with the Chromo Shadow Domain of LHP1

To gain insight into the interaction of BPC6 and LHP1, we aimed to identify the domains responsible for the heterodimerization. BPC6 consists of three distinct regions (Fig. 2A): an N-terminal dimerization domain that is responsible for the formation of homotypic dimers within group II BBR/BPC proteins, an NLS, and the highly conserved BPC DNA-binding domain (Brand et al., 2010; Wanke et al., 2011). LHP1 also consists of three principal domains (Fig. 2B): the N-terminal chromo domain, which binds to histone 3, a variable hinge region, and the chromo shadow domain (CSD) at the C terminus, which mediates protein-protein interactions (Gaudin et al., 2001; Latrasse et al., 2011).

By using truncated fusion proteins in yeast two-hybrid analyses, we could show that the group II BBR/BPC-specific Ala zipper-like dimerization domain and the C terminus of LHP1 that contains the CSD are required for the formation of the BPC6/LHP1 heterodimers (Fig. 2C). Interestingly, the subnuclear localizations of BPC6-GFP and LHP1ΔN-RFP overlapped (Supplemental Fig. S4), which suggest a recruitment of this LHP1 fragment by its CSD to BPC6 expression domains.

BPC6 Recruits LHP1 to GAGA DNA Motifs

BBR/BPC family members bind to the dinucleotide repeat sequence GAGA (Sangwan and O'Brian, 2002; Santi et al., 2003; Meister et al., 2004; Kooiker et al., 2005; Brand et al., 2010). Therefore, our data suggested that BPC6 might recruit LHP1 to GAGA motif-containing DNA. To investigate the interaction of BPC6 with LHP1 at the DNA, we adapted the DNA-protein interaction-ELISA method (Brand et al., 2010) by adding an additional round of protein incubation (Fig. 3A). This DNA-protein interaction-recruitment (DPI-R)-ELISA allowed us to investigate also those proteins that are associated with nucleic acids but do not bind DNA directly (Fig. 3A). We used the identical DNA probes that we used previously for the specific binding of BPC2 to GAGA motifs (Brand et al., 2010). The probes were immobilized in different wells and incubated with recombinant GFP-BPC6 (Fig. 3B). As expected, specific binding of GFP-BPC6 to GAGA probes was detected by GFP fluorescence. We next added 6xHis-LHP1 or 6xHis control extract to the DPI-R-ELISA (Fig. 3B). Only those wells that contained all three components, GAGA probe, GFP-BPC6, and 6xHis-LHP1, displayed significant luminescence over the background (Fig. 3B). Consistently, a DPI-R-ELISA with 6xHis-LHP1ΔN also gave significant signals and thereby confirmed the yeast two-hybrid data (Supplemental Fig. S5). Hence, BPC6 was required and sufficient to recruit LHP1 via its CSD-containing C terminus to GAGA motif-containing DNA probes in vitro.

GAGAGA Motifs Are Enriched in Known LHP1 and H3K27me3 Target Loci

Previous bioinformatics studies indicated that GAGAGA hexanucleotide motifs were enriched in core promoters, introns, and 5′ untranslated regions, especially of TATA-less genes (Santi et al., 2003; Berendzen et al.,
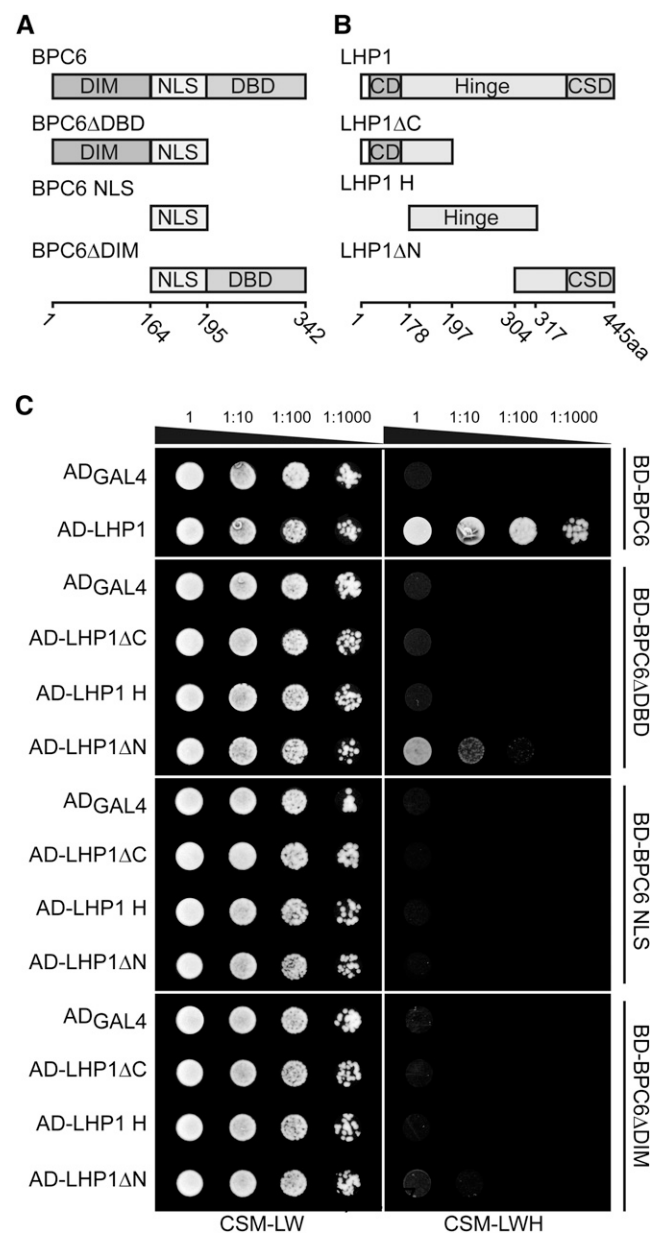

Figure 2. The dimerization domain of BPC6 physically interacts with the CSD of LHP1. A and B, Schematic overviews of the BPC6 (A) and LHP1 (B) truncations used for localization and interaction studies. DIM, Dimerization domain; DBD, DNA-binding domain; CD, chromo domain. C, Yeast two-hybrid analyses of BPC6 and LHP1 hybrid fusion proteins. The dimerization domain of BPC6 (BPC6ΔDBD) interacted exclusively with the CSD of LHP1 (LHP1ΔN). AD, Activation domain; BD, DNA-binding domain; CSM-LW, complete supplement mixture without Leu and Trp; CSM-LWH, complete supplement mixture without Leu, Trp, and His.

2006; Yamamoto et al., 2009). Moreover, GAGA/TCTC repeat motifs were discovered in promoters of genes that are important for the developmental phase shift from vegetative to generative growth (Winter et al., 2011). Based on these previous analyses, we investigated the global distribution of the GAGAGA hexanucleotide motifs at the translation start site. Indeed, a significant enrichment (5-fold; $P < 10^{-24}$) of GAGAGA close to ATG implied a role in gene expression control (Fig. 4A; Supplemental Table S1). Interestingly, we found that the GAGAGA hexanucleotide motif displayed an orientation-dependent distribution at the translation start: the antisense TCTCTC was abundant in the 5' untranslated regions and in the gene body, possibly in introns; the sense GAGAGA hexanucleotide motif was less frequent than its antisense and disclosed a sharp peak right upstream of the ATG (Fig. 4A). Due to the BPC6/LHP1 interaction, we analyzed the overlap between genes with GAGAGA in their promoters that were already known LHP1 in vivo target loci or associated with
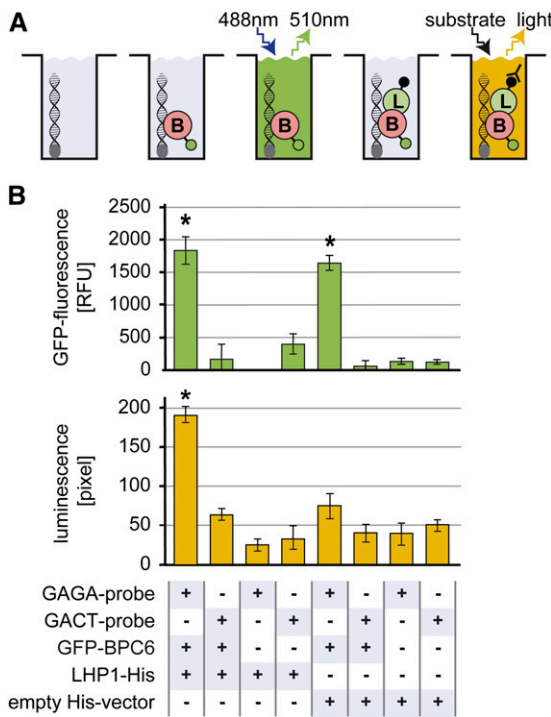

Figure 3. BPC6 recruits LHP1 to GAGA motifs in vitro. A, Schematic overview of the in vitro DPI-R-ELISA. Immobilized DNA probes were incubated with GFP-BPC6 and, subsequently, with His-LHP1 fusion proteins. The recruitment of LHP1 by BPC6 to DNA probes was detected by using anti-His antibody and quantified by relative luminescence. B, DPI-R-ELISA with recombinant GFP-BPC6 and His-LHP1. Histograms show relative GFP fluorescence (top) and luminescence (bottom). BPC6 was required and sufficient to recruit LHP1 specifically to GAGA motif-containing DNA probes in vitro. Significant signals are marked by asterisks ($P < 0.05$). Error bars indicate SE. RFU, Relative fluorescence units.
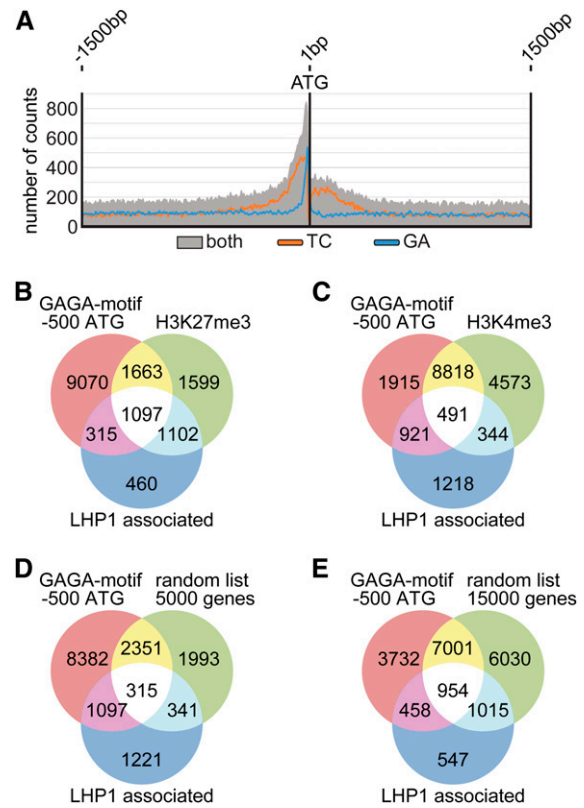

Figure 4. GAGA motifs link BPC6 function with LHP1 targets and H3K27me3. A, Distribution map of GAGAGA in a 3-kb region centered on the translation start sites (ATG). GAGA motifs were strongly enriched before the ATG. The sense (blue line) and antisense (orange line) orientations display significant positional disequilibria. B to E, Overlap of H3K27me3 (B) or histone H3 Lys-4 trimethylation (H3K4me3; C) chromatin marks or two random gene lists (D and E) with genes that contain GAGAGA motifs in their promoters and that are in vivo LHP1 targets. Statistical analysis of the gene list overlap is given in Supplemental Table S3.

distinct histone modifications (Fig. 4B; Supplemental Tables S1 and S2; Zhang et al., 2007; Lafos et al., 2011; Roudier et al., 2011; Luo et al., 2013). Interestingly, a significant overlap of genes existed at the triple intersection between GAGAGA-containing promoters, LHP1 targets, and the H3K27me3 mark (Fig. 4B; Supplemental Table S3; $P \leq 0$), although there was no significant overlap between the GAGAGA data set and any of the individual data sets. No significant enrichment was found for any other triple overlap between GAGAGA hexanucleotide motifs, LHP1 in vivo target loci, and any other histone modification (Fig. 4C; Supplemental Fig. S6; Supplemental Table S3). It is noteworthy, however, that GAGAGA hexanucleotide motifs appeared to be associated with several histone modifications but was absent in control lists of random gene composition (Fig. 4, D and E; Supplemental Fig. S6; Supplemental Table S3). These observations might relate to the roles of group I or III BBR/BPC proteins or to other, yet unknown group II BBR/BPC functions that are LHP1 independent.

The *lhp1-4 bpc4 bpc6* Mutant Displays Severe Pleiotropic Developmental Defects

To investigate the biological relevance of the interaction between group II BBR/BPCs and LHP1, we crossed the previously described *bpc4 bpc6* double mutant with *lhp1-4* (Larsson et al., 1998; Lindroth et al., 2004; Monfared et al., 2011). We observed a much lower allele penetrance for early-flowering *lhp1-4* and for the *lhp1-4 bpc4 bpc6* triple mutant than was expected: we screened a total of 980 F2 plants and, therefore, expected 240 homozygous early-flowering *lhp1-4* plants and 15 triple mutant genotypes. In vast contrast, 118 homozygous *lhp1-4* plants (twice less than expected) and only a single *lhp1-4 bpc4 bpc6* triple mutant (16 times less than expected; $\chi^2 < 10^{-10}$) were observed (Supplemental Table S4).

The *lhp1-4 bpc4 bpc6* triple mutant exhibited severe pleiotropic defects: the mutant plants were smaller in size, exhibited fewer side shoots, and had an altered number of branches of the main inflorescence compared with the wild type or both parental lines (Fig. 5A). We observed smaller flowers in all three mutant alleles and missing floral organs in *lhp1-4 bpc4 bpc6*

(Fig. 5B). Even though some aborted seeds in *bpc4 bpc6* were observed (Fig. 5C), the silique size and the number of seeds per silique were not significantly altered (Fig. 5D). However, the size of the siliques and the number of seeds were reduced in *lhp1-4* or *lhp1-4 bpc4 bpc6* (Fig. 5, C and D). Rosette leaves of *lhp1-4 bpc4 bpc6* plants were drastically altered in size and form (Fig. 5E). We also observed a reduced number of rosette leaves in all three mutant alleles, which was indicative of an early-flowering phenotype and strongest in the *lhp1-4 bpc4 bpc6* triple mutant (Fig. 5F). Consistent with the reduced rosette leaf number, *lhp1-4 bpc4 bpc6* flowered significantly earlier (1–2 d; $\chi^2 < 10^{-5}$) than *lhp1-4* and much earlier (approximately 12 d; $\chi^2 < 10^{-99}$) than *bpc4 bpc6* or wild-type plants (Fig. 5G).

Synergistic Control of Gene Expression by Group II BBR/BPCs and LHP1

We further analyzed the genetic interaction between LHP1 and BPC6 by comparing the transcriptomes of *bpc4 bpc6*, *lhp1-4*, *lhp1-4 bpc4 bpc6*, and wild-type plants. A total of 723 genes displayed at least a 3-fold
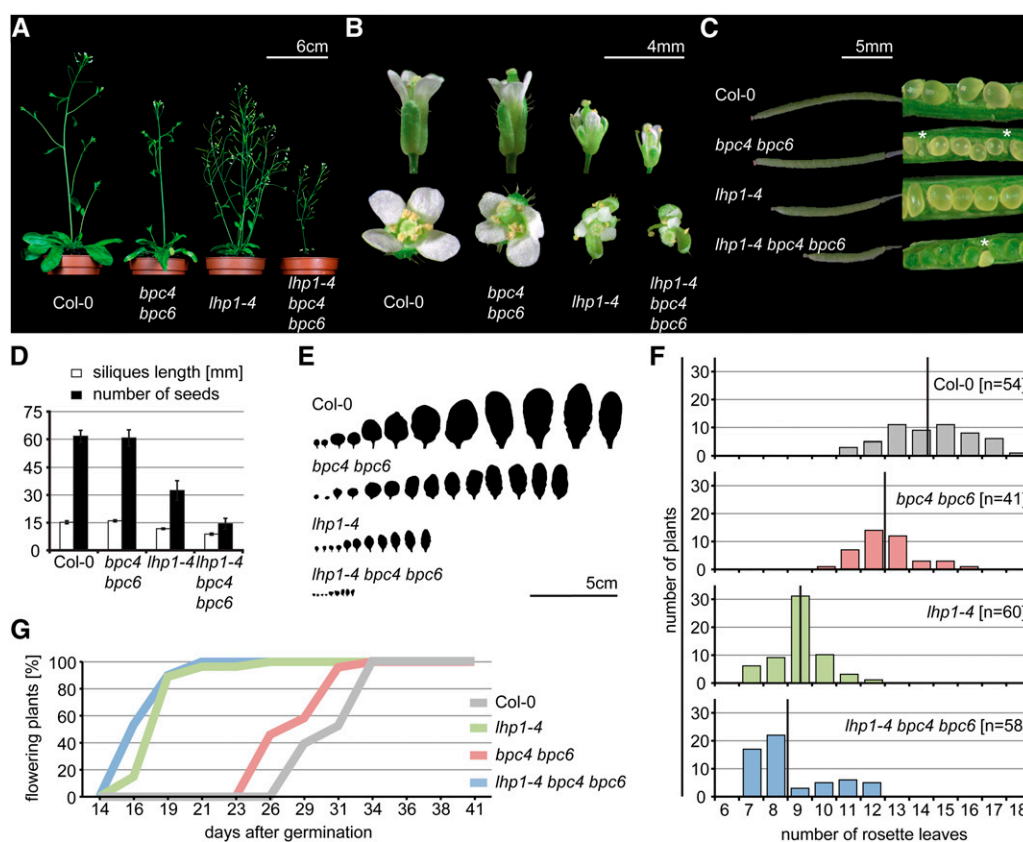

Figure 5. The triple mutant of group II BPCs and LHP1 displays severe pleiotropic defects. A, Plant growth habit. B, Flower morphology. C, Silique morphology (left) and seed set (right). Aborted and dying seeds are marked by asterisks. D, Length of siliques and number of seeds per silique. Error bars indicate SD. E, Silhouettes of rosette leaves at the time of bolting. F, Total number of rosette leaves at bolting stage. The average number of rosette leaves is indicated by black vertical lines. G, Flowering time given as relative number of plants at bolting stage. Col-0, Accession Columbia-0.

difference in expression in at least one of the mutant genotypes compared with the wild type (Fig. 6A; Supplemental Table S5). Only 17 genes were differentially expressed in all three genotypes (Fig. 6A). A vast majority of 660 DE genes were found in *lhp1-4 bpc4 bpc6* alone, which was many more than in the two parental genotypes. Moreover, 412 DE genes were misexpressed exclusively in *lhp1-4 bpc4 bpc6*. This gene expression pattern could not be proposed from the DE genes in the parental plants and explicitly supported a synergistic interaction between group II BBR/BPCs and LHP1. To disclose the biological processes in which LHP1 and group II BBR/BPCs were involved, we investigated the Gene Ontology terms of all DE genes (Supplemental Table S6). A significant enrichment in the Gene Ontology terms nucleotide binding (molecular function), transcription factor activity (molecular function), and response to stress (biological processes) was found (Supplemental Fig. S7). Consistently, many TF genes were misexpressed in *lhp1-4* and *lhp1-4 bpc4 bpc6* (Fig. 6B), and a significant overlap of all DE genes with known H3K27me3 targets (Lafos et al., 2011) in the shoot was disclosed (Fig. 6C). In agreement with an overall repressive function of LHP1 or H3K27me3, more genes were up-regulated than down-regulated in all mutants (Fig. 6D; Supplemental Table S5). In addition, a significant overlap between up-regulated genes, GAGAGA hexanucleotide motifs in promoters, and known H3K27me3 targets was observed in all three mutants (Fig. 6D).

Several well-known homeotic TFs were under synergistic control of both LHP1 and group II BPCs (Fig. 6E; Supplemental Table S5). We analyzed a few candidate TFs that were already known in vivo LHP1 targets (Zhang et al., 2007), repressed by H3K27me3 marks in the shoot (Lafos et al., 2011), and simultaneously contained GAGAGA hexanucleotide motifs in the proximal promoters 500 bp upstream of the ATG. The homeotic MADS box genes *AGAMOUS*, *SHATTERPROOF1* (*SHP1*), *SHP2*, and *SEPALLATA2* (Fig. 6E; Supplemental Table S5) displayed a much more pronounced misexpression in *lhp1-4 bpc4 bpc6* compared with the parental mutants, which also confirms a synergistic interaction of LHP1 and group II BPCs at these homeotic TF genes. Ectopic derepression of any of these TFs in the shoot tissues harbors the potential of homeotic transformations that might already explain much of the observed phenotypic differences in *lhp1-4 bpc4 bpc6* mutants (Ferrándiz et al., 2000; Pelaz et al., 2000; Liu et al., 2009; Colombo et al., 2010). The early-flowering phenotype of *lhp1-4* was proposed to result from the high expression of *FLOWERING LOCUS T* (Kotake et al., 2003), which was even higher expressed in the triple mutant than in *lhp1-4*. Still, many more TF genes with homeotic potential were overexpressed and probably contribute to the severity of the *lhp1-4 bpc4 bpc6* phenotype. For example, *HOMEOBOX PROTEIN2*, *MYB23*, and *BELLRINGER/BEL1-LIKE HOMEODOMAIN9* were all under the synergistic control of LHP1 and group II BBR/BPC proteins, contain GAGAGA hexanucleotide

motifs in their promoters, and are LHP1 target loci. Similar deregulation was found for *ACC OXIDASE*, *SMALL AUXIN UPREGULATED36*, and *BTB AND TAZ DOMAIN PROTEIN2*, which are involved in phytohormone signaling, or *ARABIDOPSIS DEHISCENCE ZONE POLYGALACTURONASE1*, which encodes an indispensable enzyme for proper cell separation during reproductive development (Fig. 6E).

Interestingly, the expression of known group I BBR/BPC targets such as *LEC2*, *INO*, *STK*, or *BP/KNAT1* was not significantly affected in *bpc4 bpc6* or *lhp1-4 bpc4 bpc6*, which was a strong indication for distinct functionalities of the two groups of BBR/BPC proteins (Supplemental Fig. S8).

DISCUSSION

In this work, we have shown that the plant group II BBR/BPC protein BPC6 was able to recruit LHP1, a plant PRC1 component, to GAGA motif-containing DNA elements. Consistently, bioinformatics analysis revealed that GAGA motifs were significantly enriched at genomic LHP1 in vivo target sites and at regions with increased H3K27me3.

Our FLIM analyses indicated that the BPC6/LHP1 heterocomplex is in close proximity with the PRC2 member VRN2 in vivo. These data suggest a novel function for group II BBR/BPC proteins in H3K27me3 repression via LHP1, which directly interacts with VRN2 and other PRC2 components that are required for setting the H3K27me3 marks.

Previous publications suggested that BBR/BPC family members might function through plant PRE-like elements to influence the expression of homeotic genes (Santi et al., 2003; Schatlowski et al., 2008). In animals, PREs were defined by their importance for gene repression by PcG proteins (Schwartz and Pirrotta, 2008). Previous bioinformatics analyses of the in vivo target loci of the PRC2 member FIE identified an enrichment of GAGA motifs at putative PRE-like elements (Deng et al., 2013). Our work directly supports the existence of such PRE-like elements in plants by identifying a DNA-binding protein, BPC6, that can mediate the specific interaction of the PRC1 component LHP1 with GAGA DNA motifs.

In recent years, several LHP1-interacting proteins were identified, which suggested roles in many chromatin complexes like HP1 in animals (Gaudin et al., 2001; Cui and Benfey, 2009; del Olmo et al., 2010; Kwon and Workman, 2011; Latrasse et al., 2011; Li and Luan, 2011; Derkacheva et al., 2013; Molitor and Shen, 2013; Shen et al., 2014). For example, LHP1 interacts with SCARECROW (SCR), a member of the plant-specific GRAS transcription factor family, which affects cell division in the roots (Cui and Benfey, 2009). However, no direct evidence for PRE-like elements at SCR and LHP1 targets was disclosed. Similarly, no direct link with DNA elements could be suggested for the interaction between LHP1 and RING-finger
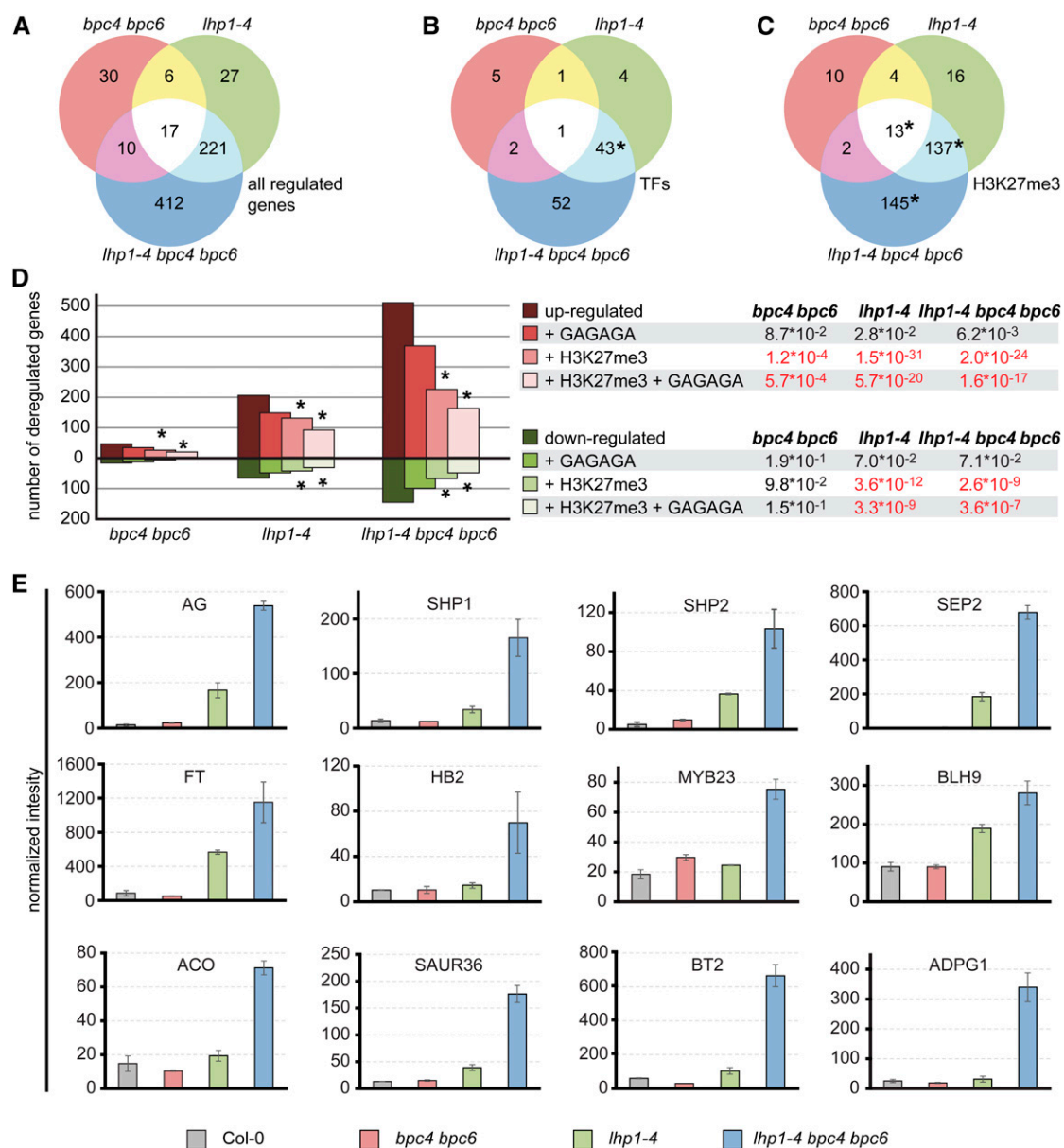
Figure 6. Synergistic interaction between group II BBRs/BPCs and LHP1. A, Overlap of DE genes. B, Overlap of DE TF genes (Guo et al., 2005). *, $P \leq 10^{-4}$. C, Overlap of DE genes that are known H3K27me3 target loci (Lafos et al., 2011). *, $P \leq 10^{-4}$. D, Number of up- or down-regulated genes that contain GAGAGA hexanucleotide motifs in their promoters ($-1,500$ bp to ATG) and/or are H3K27me3 decorated. For each combination, the hypergeometric P value is given. Red values indicate significant enrichment. E, Examples of synergistically regulated genes that are in vivo LHP1 and H3K27me3 targets and contain GAGA motifs in their promoters. Top row, MADS box genes; middle row, homeotic TF genes; bottom row, other genes with importance in development. Background corrected signal intensities are shown. Error bars indicate SE. Col-0, Accession Columbia-0; AG, *AGAMOUS*; SEP2, *SEPALLATA2*; FT, *FLOWERING LOCUS T*; HB2, *HOMEOBOX PROTEIN2*; BLH9, *BELLRINGER/BEL1-LIKE HOMEODOMAIN9*; ACO, *ACC OXIDASE*; SAUR36, *SMALL AUXIN UPREGULATED36*; BT2, *BTB AND TAZ DOMAIN PROTEIN2*; ADPG1, *ARABIDOPSIS DEHISCENCE ZONE POLYGALACTURONASE1*.

proteins, which are essential for the plant PRC1 complex and monoubiquitination of histone H2A (Xu and Shen, 2008; Liu et al., 2009; Bratzel et al., 2010; Molitor and Shen, 2013; Calonje, 2014; Feng and Shen, 2014). The recruitment of LHP1 by BPC6 to GAGA DNA motifs is reminiscent of the animal process, where the Trl GAF can participate in histone modifications and

gene silencing through its binding to PRC1 components (Faucheux et al., 2003; Mulholland et al., 2003; Salvaing et al., 2003).

It remains unclear, however, how group II BBR/BPCs target a specific GAGA motif, which is short and highly abundant in the genome (Santi et al., 2003; Berendzen et al., 2006). It was proposed that the

homotypic dimerization of group II BBR/BPC proteins and their parallel dimer facilitates binding to neighboring GAGA sites and, therefore, may participate in the binding specificity in vivo (Wanke et al., 2011). Most plausible is the organization of GAGA motifs in a cis-regulatory module with other binding motifs (e.g. LEAFY binding sites; Winter et al., 2011). Hence, group II BBR/BPC members may identify the correct plant PRE-like elements in concert with other TFs or possibly group I BBR/BPCs (Berger et al., 2011; Winter et al., 2011).

The phenotypic analysis of the *lhp1-4 bpc4 bpc6* triple mutant suggested a synergistic interaction between group II BBR/BPC proteins and LHP1. These data were supported by our transcriptome analyses, which uncovered that, for instance, important developmental regulators were under synergistic control. This synergy might be explained by an involvement of both proteins in different pathways (e.g. the pleiotropic function of LHP1 with its multiple partners might contribute at very different levels to this synergy and to the triple mutant phenotype). Similarly, BPC6 homodimers might also act by a different molecular mechanism that is independent of LHP1 on gene expression control of common target genes.

Despite the importance of group II BBR/BPCs for LHP1, the *bpc4 bpc6* double mutant displays a rather mild phenotype (Monfared et al., 2011). These subtle phenotypic changes can possibly be explained by the expression of a partial *BPC4* fragment from the transfer DNA (T-DNA) insertion locus in *bpc4 bpc6* plants (Supplemental Fig. S9). Unfortunately, this *bpc4* allele is currently the only available line where the *BPC4* coding sequence is affected by the insertion. The T-DNA integrated into the reading frame of the DNA-binding domain coding part of the gene (Supplemental Fig. S10); thus, the truncated BPC4 protein will not bind to DNA anymore but can probably form homodimers and may interact with LHP1 or other unknown interaction partners. In addition, group I and group II BBR/BPC members might possibly compete for binding to GAGA motifs in similar and partially overlapping gene targets. Therefore, it might be possible that group I BBR/BPC proteins can partially complement the repressive group II function at some vacant GAGA loci in *bpc4 bpc6* plants independently of PcG members via the SEU/LUG suppressor complex, which presumably acts through a different mechanism (Simonini et al., 2012; Lee et al., 2014).

Our in vivo data suggested that probably a BPC6 dimer binds to DNA and recruits LHP1 via its CSD to form a scaffold for VRN2. Hence, group II BBR/BPC proteins may also be involved in the orchestration of the deposition of H3K27me3, as was proposed earlier (Santi et al., 2003; Schatlowski et al., 2008). However, we missed so far the catalytic component that is responsible for the histone methylation. In addition, our in vivo FLIM analyses have certain limitations, and some tested components, such as the histone methyltransferaseses CURLY LEAF and SWN or FIE and MSI1, might also be associated with the BPC6/LHP1

complex but remained cryptic in our analyses, as they were not close enough to evoke a significant change in GFP donor lifetime (Wanke et al., 2011; Harter et al., 2012). Therefore, much more time-resolved investigations will be required to decipher the precise series of events in the mechanism of BPC6/LHP1 function. Interestingly, in the leaf meristems, a recruitment of PRC2 to specific DNA motifs is facilitated by the ASYMMETRIC LEAVES (AS) complex to maintain the repression of *KNOX* homeobox genes (Lodha et al., 2013). The AS/PRC2-dependent process is supposed to operate locally and only during a defined developmental phase. The possible BPC6/LHP1-dependent recruitment of certain PRC2 members may act in a similar way on a presumably different subset of genes. Further analyses will be required to clarify the extent to which any of the other VRN2 paralogs in Arabidopsis can also be incorporated into a possible BPC6/LHP1-dependent complex.

Thus, we propose a possible model for BPC6 function during PRC-dependent gene silencing (Fig. 7). Group II BBR/BPC proteins recruit LHP1 to certain GAGA motifs in the promoters of a subset of homeotic genes. VRN2 bound to BPC6/LHP1 might participate in the functions of VRN2-PRC2 to initiate, maintain, spread, or reinforce a silent chromatin state. A similar model was proposed for the inheritance of epigenetic information through mitotic cell division that involves LHP1 and MSI1 (Derkacheva et al., 2013). It might also be possible that group II BBR/BPCs, PRC1 and PRC2 members, participate together in the same complex at GAGA motif-containing PREs. This concept is consistent with a function of the PRC2 member FIE in a possible BBR/BPC-dependent H3K27me3 at plant PRE-like elements (Deng et al., 2013).

Although our model envisions a role for BPC6, LHP1, and possibly other PRC1 and PRC2 members during the initial phase of gene silencing, it is not at all conflicting with our knowledge that led to the classic hierarchical model. Moreover, this model combines our data with previous findings on the importance of PRC1 in setting the H3K27me3 marks at distinct genomic loci (Derkacheva et al., 2013; Yang et al., 2013). Still, various models might exist in parallel with other forms of PRC recruitment and repression yet to be uncovered.
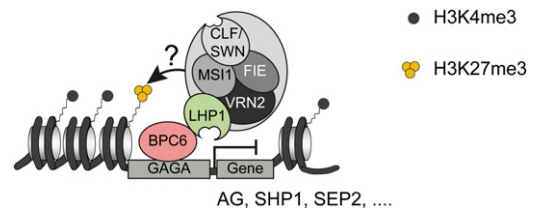

Figure 7. Model for synergistic BPC6 and LHP1 function during the initial phase of PRC2-dependent gene silencing at distinct homeotic gene loci. BPC6 binds to GAGA motifs in PRE-like DNA elements and recruits LHP1. Both proteins form a scaffold for the sequential attachment of VRN2 and other PRC2 members. AG, *AGAMOUS*; H3K4me3, histone H3 Lys-4 trimethylation; SEP2, *SEPALLATA2*.

CONCLUSION

Our study revealed that the plant GAGA-binding protein BPC6 recruits LHP1 and probably VRN2 to GAGA motif-containing PRE-like DNA elements in plants. In animals, the GAF proteins Trl and Psq act in the recruitment of PcG members to specific PREs (Adkins et al., 2006; Schuettengruber and Cavalli, 2009, 2013). Hence, the group II BBR/BPC function resembles animal GAFs in their role in PRC1 recruitment. It is noteworthy that animal and plant GAFs do not share any sequence similarities despite their high degree of molecular mechanistic analogy (Wanke et al., 2011), which, therefore, must have evolved independently through convergent evolution.

MATERIALS AND METHODS

Yeast Two-Hybrid Analysis

The protocol of yeast (*Saccharomyces cerevisiae*) two-hybrid assays was described previously (Wanke et al., 2011). Matchmaker (Clontech)-compatible pGBKT7-DEST and pGADT7-DEST vectors were recombined with corresponding entry clones and transformed to the PJ69-4A yeast strain. Complementation of auxotrophy was scored by growth on selective medium.

Image-Capture Analysis and Optical Spectroscopic Measurements

Confocal laser scanning microscopy was performed using the Leica TCS SP2 or SP8 confocal microscope (Leica Microsystems). BiFC and FLIM were performed in transiently transformed *Nicotiana benthamiana* leaf epidermis cells according to Schütze et al. (2009) and Wanke et al. (2011). The presence of yellow fluorescent protein fluorescence was scored 1 to 2 d post infiltration. Expression of the correct fusion proteins was tested by western-blot analyses with antibodies against the fluorophores. Confocal laser scanning microscopy image capture and analysis were described previously (Wanke et al., 2011). Förster resonance energy transfer-FLIM was performed either with a custom-built confocal stage scanning microscope, as described previously (Elgass et al., 2010; Wanke et al., 2011) or with an SP8 confocal microscope equipped with a FLIM unit and the Leica Application Suite Advanced Fluorescence analysis suite (Leica Microsystems). FLIM data on display are derived from three to nine different biological replicates/independent transformations and measurements of five to 10 cells each.

Protein Expression and DPI-R-ELISA

Protein expression, isolation, and western-blot analysis were performed as described previously (Brand et al., 2010, 2013). The DPI-R-ELISA was performed essentially as the previously described DNA-protein interaction ELISA for BPC2-His (Brand et al., 2010) but was extended for an additional round of incubation. DNA binding of recombinant GFP-BPC6 was detected by fluorescence measurements. Subsequently, recombinant 6xHis-LHP1, 6xHis-LHP1ΔN, or His control was added. Successful recruitment was investigated immunologically with anti-His-horseradish peroxidase antibodies and luminescence substrate reaction. Recombinant proteins in the extracts were detected by immunoblotting (Supplemental Fig. S4, B and C).

Phenotypic Analysis and Plant Growth Conditions

Arabidopsis (*Arabidopsis thaliana*) genotypes (accession Columbia-0) were cultivated in the greenhouse with supplemental lighting (temperature, day 20°C/night 19°C; humidity, 35%; 18 h of light/6 h of dark). The *bpc4 bpc6* mutant line was provided by C.S. Gasser (Monfared et al., 2011). To isolate homozygous triple mutants, PCR-based genotyping and phenotypic preselection were combined. Segregation and differences in bolting of the mutant phenotypes were analyzed by χ^2 test. Gene-specific and/or T-DNA border primers

were used to verify the mutant genotypes (Supplemental Fig. S10). To compare flowering time and number of rosette leaves, plants of all genotypes were cultivated in the greenhouse (Supplemental Fig. S11). At the time of bolting, the number of rosette leaves was counted.

Microarray Hybridization and Data Processing

Plants were grown in the greenhouse and harvested 18 d after germination. Plant material was pooled and stored at −80°C for further analysis. Up to nine individual plants were pooled per biological replicate. Two replicates per genotype were used for ATH1 GeneChip (Affymetrix) analyses. Sample preparation, copy RNA synthesis, and quality controls were performed as described before (Wenke et al., 2012). The Affymetrix CEL files were imported into GeneSpring GX software version 7.3 (Agilent Technologies). The microarray data from this article have been submitted to the National Center for Biotechnology Information Gene Expression Omnibus and assigned the identifier GSE68437. Normalization, background correction, and comparison of replicates were performed as described before (Kilian et al., 2007). Signal intensities of both treatment replicates that were at least 3-fold higher or lower than the signal intensities for both control replicates were classified as up- or down-regulated, respectively. Processed microarray data on DE genes are provided as Supplemental Table S5.

Functional categorization using Gene Ontology terms was performed at The Arabidopsis Information Resource (http://www.arabidopsis.org) with genome release 9. The data for H3K27me3 in vivo targets were taken from Lafos et al. (2011) and Luo et al. (2013), and the data for any other histone marks were taken from Roudier et al. (2011) and Luo et al. (2012). In vivo targets of LHP1 were taken from Zhang et al. (2007). Significant gene list overlap between data sets was calculated using the hypergeometric distribution in the R statistical environment of Bioconductor (http://www.r-project.org/): each side of the probability distribution was tested independently for underrepresentation {sum[dhyper(1:x, m, $N − m$, k)]} or overrepresentation {sum[dhyper(x:k, m, $N − m$, k)]}, where N is the size of the population with m the number of incidents within the population and k is the size of the sample with x as the number of incidents within the sample.

The Arabidopsis Genome Initiative identifiers for the genes and proteins used in this article are as follows: BPC6, AT5G42520; LHP1, AT5G17690; SWN, AT4G02020; FAS2, AT5G64630; FIE, AT3G20740; MSI1, AT5G58230; and VRN2, AT4G16845.

Supplemental Data

The following supplemental materials are available.

Supplemental Figure S1. BPCs colocalize with the tested PRC2 and PRC1 core components.

Supplemental Figure S2. BPC6-GFP interacts with LHP1-RFP and BPC6-RFP in vivo.

Supplemental Figure S3. BPC4 interacts with LHP1.

Supplemental Figure S4. BPCs colocalize with LHP1 truncations.

Supplemental Figure S5. DPI-R-ELISA with GFP-BPC6 and 6xHis-LHP1ΔN.

Supplemental Figure S6. Comparison of genes with GAGAGA motifs in their promoters, LHP1 in vivo target loci, and different chromatin marks.

Supplemental Figure S7. Gene ontology analysis of differentially expressed genes.

Supplemental Figure S8. Differentially expressed genes.

Supplemental Figure S9. Expression trajectories of *BPC4*, *BPC6*, and *LHP1* in the mutant genotypes.

Supplemental Figure S10. PCR-based genotyping of the T-DNA insertion in *bpc4 bpc6* and *lhp1-4 bpc4 bpc6*.

Supplemental Figure S11. Phenotype of 21-d-old plants.

Supplemental Table S1. List of GAGAGA motif-containing gene loci.

Supplemental Table S2. Random gene lists.

Supplemental Table S3. Statistical analysis of gene list overlap between GAGAGA motif-containing genes, LHP1 in vivo targets, and chromatin marks.

Supplemental Table S4. Segregation analysis of the F2 generation of *lhp1-4 bpc4 bpc6* mutants.

Supplemental Table S5. List of all up- and down-regulated genes.

Supplemental Table S6. Gene ontology analysis of all differentially expressed genes.

ACKNOWLEDGMENTS

LITERATURE CITED

Adkins NL, Hagerman TA, Georgel P (2006) GAGA protein: a multi-faceted transcription factor. Biochem Cell Biol 84: 559–567

Badis G, Berger MF, Philippakis AA, Talukder S, Gehrke AR, Jaeger SA, Chan ET, Metzler G, Vedenko A, Chen X, et al (2009) Diversity and complexity in DNA recognition by transcription factors. Science 324: 1720–1723

Berendzen KW, Stüber K, Harter K, Wanke D (2006) Cis-motifs upstream of the transcription and translation initiation sites are effectively revealed by their positional disequilibrium in eukaryote genomes using frequency distribution curves. BMC Bioinformatics 7: 522

Berger N, Dubreucq B, Roudier F, Dubos C, Lepiniec L (2011) Transcriptional regulation of *Arabidopsis LEAFY COTYLEDON2* involves RLE, a *cis*-element that regulates trimethylation of histone H3 at lysine-27. Plant Cell 23: 4065–4078

Brand LH, Henneges C, Schüssler A, Kolukisaoglu HU, Koch G, Wallmeroth N, Hecker A, Thurow K, Zell A, Harter K, et al (2013) Screening for protein-DNA interactions by automatable DNA-protein interaction ELISA. PLoS ONE 8: e75177

Brand LH, Kirchler T, Hummel S, Chaban C, Wanke D (2010) DPI-ELISA: a fast and versatile method to specify the binding of plant transcription factors to DNA in vitro. Plant Methods 6: 25

Bratzel F, López-Torrejón G, Koch M, Del Pozo JC, Calonje M (2010) Keeping cell identity in Arabidopsis requires PRC1 RING-finger homologs that catalyze H2A monoubiquitination. Curr Biol 20: 1853–1859

Buzas DM, Tamada Y, Kurata T (2012) FLC: a hidden polycomb response element shows up in silence. Plant Cell Physiol 53: 785–793

Calonje M (2014) PRC1 marks the difference in plant PcG repression. Mol Plant 7: 459–471

Cedar H, Bergman Y (2009) Linking DNA methylation and histone modification: patterns and paradigms. Nat Rev Genet 10: 295–304

Colombo M, Brambilla V, Marcheselli R, Caporali E, Kater MM, Colombo L (2010) A new role for the SHATTERPROOF genes during Arabidopsis gynoecium development. Dev Biol 337: 294–302

Cui H, Benfey PN (2009) Interplay between SCARECROW, GA and LIKE HETEROCHROMATIN PROTEIN 1 in ground tissue patterning in the Arabidopsis root. Plant J 58: 1016–1027

del Olmo I, López-González L, Martín-Trillo MM, Martínez-Zapater JM, Piñeiro M, Jarillo JA (2010) EARLY IN SHORT DAYS 7 (ESD7) encodes the catalytic subunit of DNA polymerase epsilon and is required for flowering repression through a mechanism involving epigenetic gene silencing. Plant J 61: 623–636

Deng W, Buzas DM, Ying H, Robertson M, Taylor J, Peacock WJ, Dennis ES, Helliwell C (2013) Arabidopsis Polycomb Repressive Complex 2 binding sites contain putative GAGA factor binding motifs within coding regions of genes. BMC Genomics 14: 593

Derkacheva M, Steinbach Y, Wildhaber T, Mozgová I, Mahrez W, Nanni P, Bischof S, Gruissem W, Hennig L (2013) Arabidopsis MSI1 connects LHP1 to PRC2 complexes. EMBO J 32: 2073–2085

Elgass K, Caesar K, Wanke D, Harter K, Meixner AJ, Schleifenbaum F (2010) Application of FLIM-FIDSAM for the in vivo analysis of hormone competence of different cell types. Anal Bioanal Chem 398: 1919–1925

Faucheux M, Roignant JY, Netter S, Charollais J, Antoniewski C, Théodore L (2003) batman interacts with polycomb and trithorax group genes and

encodes a BTB/POZ protein that is included in a complex containing GAGA factor. Mol Cell Biol 23: 1181–1195

Feng J, Shen WH (2014) Dynamic regulation and function of histone monoubiquitination in plants. Front Plant Sci 5: 83

Ferrándiz C, Liljegren SJ, Yanofsky MF (2000) Negative regulation of the SHATTERPROOF genes by FRUITFULL during Arabidopsis fruit development. Science 289: 436–438

Gaudin V, Libault M, Pouteau S, Juul T, Zhao G, Lefebvre D, Grandjean O (2001) Mutations in LIKE HETEROCHROMATIN PROTEIN 1 affect flowering time and plant architecture in Arabidopsis. Development 128: 4847–4858

Guo A, He K, Liu D, Bai S, Gu X, Wei L, Luo J (2005) DATF: a database of Arabidopsis transcription factors. Bioinformatics 21: 2568–2569

Harter K, Meixner AJ, Schleifenbaum F (2012) Spectro-microscopy of living plant cells. Mol Plant 5: 14–26

Huang DH, Chang YL, Yang CC, Pan IC, King B (2002) pipsqueak encodes a factor essential for sequence-specific targeting of a polycomb group protein complex. Mol Cell Biol 22: 6261–6271

Kasinathan S, Orsi GA, Zentner GE, Ahmad K, Henikoff S (2014) High-resolution mapping of transcription factor binding sites on native chromatin. Nat Methods 11: 203–209

Kilian J, Whitehead D, Horak J, Wanke D, Weinl S, Batistic O, D'Angelo C, Bornberg-Bauer E, Kudla J, Harter K (2007) The AtGenExpress global stress expression data set: protocols, evaluation and model data analysis of UV-B light, drought and cold stress responses. Plant J 50: 347–363

Kooiker M, Airoldi CA, Losa A, Manzotti PS, Finzi L, Kater MM, Colombo L (2005) BASIC PENTACYSTEINE1, a GA binding protein that induces conformational changes in the regulatory region of the homeotic *Arabidopsis* gene SEEDSTICK. Plant Cell 17: 722–729

Kotake T, Takada S, Nakahigashi K, Ohto M, Goto K (2003) Arabidopsis TERMINAL FLOWER 2 gene encodes a heterochromatin protein 1 homolog and represses both FLOWERING LOCUS T to regulate flowering time and several floral homeotic genes. Plant Cell Physiol 44: 555–564

Kwon SH, Workman JL (2011) The changing faces of HP1: from heterochromatin formation and gene silencing to euchromatic gene expression: HP1 acts as a positive regulator of transcription. BioEssays 33: 280–289

Lafos M, Kroll P, Hohenstatt ML, Thorpe FL, Clarenz O, Schubert D (2011) Dynamic regulation of H3K27 trimethylation during Arabidopsis differentiation. PLoS Genet 7: e1002040

Lang D, Weiche B, Timmerhaus G, Richardt S, Riaño-Pachón DM, Corrêa LG, Reski R, Mueller-Roeber B, Rensing SA (2010) Genome-wide phylogenetic comparative analysis of plant transcriptional regulation: a timeline of loss, gain, expansion, and correlation with complexity. Genome Biol Evol 2: 488–503

Larsson AS, Landberg K, Meeks-Wagner DR (1998) The TERMINAL FLOWER2 (TFL2) gene controls the reproductive transition and meristem identity in Arabidopsis thaliana. Genetics 149: 597–605

Latrasse D, Germann S, Houba-Hérin N, Dubois E, Bui-Prodhomme D, Hourcade D, Juul-Jensen T, Le Roux C, Majira A, Simoncello N, et al (2011) Control of flowering and cell fate by LIF2, an RNA binding partner of the polycomb complex component LHP1. PLoS ONE 6: e16592

Lee JE, Lampugnani ER, Bacic A, Golz JF (2014) SEUSS and SEUSS-LIKE 2 coordinate auxin distribution and KNOXI activity during embryogenesis. Plant J 80: 122–135

Lehmann M (2004) Anything else but GAGA: a nonhistone protein complex reshapes chromatin structure. Trends Genet 20: 15–22

Li H, Luan S (2011) The cyclophilin AtCYP71 interacts with CAF-1 and LHP1 and functions in multiple chromatin remodeling processes. Mol Plant 4: 748–758

Li HB, Ohno K, Gui H, Pirrotta V (2013) Insulators target active genes to transcription factories and polycomb-repressed genes to polycomb bodies. PLoS Genet 9: e1003436

Libault M, Tessadori F, Germann S, Snijder B, Fransz P, Gaudin V (2005) The Arabidopsis LHP1 protein is a component of euchromatin. Planta 222: 910–925

Lindroth AM, Shultis D, Jasencakova Z, Fuchs J, Johnson L, Schubert D, Patnaik D, Pradhan S, Goodrich J, Schubert I, et al (2004) Dual histone H3 methylation marks at lysines 9 and 27 required for interaction with CHROMOMETHYLASE3. EMBO J 23: 4286–4296

Liu C, Xi W, Shen L, Tan C, Yu H (2009) Regulation of floral patterning by flowering time genes. Dev Cell 16: 711–722

Lodha M, Marco CF, Timmermans MC (2013) The ASYMMETRIC LEAVES complex maintains repression of KNOX homeobox genes via direct recruitment of Polycomb-repressive complex2. Genes Dev 27: 596–601

Luo C, Sidote DJ, Zhang Y, Kerstetter RA, Michael TP, Lam E (2013) Integrative analysis of chromatin states in Arabidopsis identified potential regulatory mechanisms for natural antisense transcript production. Plant J 73: 77–90

Meister RJ, Williams LA, Monfared MM, Gallagher TL, Kraft EA, Nelson CG, Gasser CS (2004) Definition and interactions of a positive regulatory element of the Arabidopsis INNER NO OUTER promoter. Plant J 37: 426–438

Mishra K, Chopra VS, Srinivasan A, Mishra RK (2003) Trl-GAGA directly interacts with lola like and both are part of the repressive complex of Polycomb group of genes. Mech Dev 120: 681–689

Molitor A, Shen WH (2013) The polycomb complex PRC1: composition and function in plants. J Genet Genomics 40: 231–238

Monfared MM, Simon MK, Meister RJ, Roig-Villanova I, Kooiker M, Colombo L, Fletcher JC, Gasser CS (2011) Overlapping and antagonistic activities of BASIC PENTACYSTEINE genes affect a range of developmental processes in Arabidopsis. Plant J 66: 1020–1031

Mulholland NM, King IF, Kingston RE (2003) Regulation of Polycomb group complexes by the sequence-specific DNA binding proteins Zeste and GAGA. Genes Dev 17: 2741–2746

O'Meara MM, Simon JA (2012) Inner workings and regulatory inputs that control Polycomb repressive complex 2. Chromosoma 121: 221–234

Pelaz S, Ditta GS, Baumann E, Wisman E, Yanofsky MF (2000) B and C floral organ identity functions require SEPALLATA MADS-box genes. Nature 405: 200–203

Rohs R, West SM, Sosinsky A, Liu P, Mann RS, Honig B (2009) The role of DNA shape in protein-DNA recognition. Nature 461: 1248–1253

Roudier F, Ahmed I, Bérard C, Sarazin A, Mary-Huard T, Cortijo S, Bouyer D, Caillieux E, Duvernois-Berthet E, Al-Shikhley L, et al (2011) Integrative epigenomic mapping defines four main chromatin states in Arabidopsis. EMBO J 30: 1928–1938

Salvaing J, Lopez A, Boivin A, Deutsch JS, Peronnet F (2003) The Drosophila Corto protein interacts with Polycomb-group proteins and the GAGA factor. Nucleic Acids Res 31: 2873–2882

Sangwan I, O'Brian MR (2002) Identification of a soybean protein that interacts with GAGA element dinucleotide repeat DNA. Plant Physiol 129: 1788–1794

Santi L, Wang Y, Stile MR, Berendzen K, Wanke D, Roig C, Pozzi C, Müller K, Müller J, Rohde W, et al (2003) The GA octodinucleotide repeat binding factor BBR participates in the transcriptional regulation of the homeobox gene Bkn3. Plant J 34: 813–826

Schatlowski N, Creasey K, Goodrich J, Schubert D (2008) Keeping plants in shape: polycomb-group genes and histone methylation. Semin Cell Dev Biol 19: 547–553

Schuettengruber B, Cavalli G (2009) Recruitment of polycomb group complexes and their role in the dynamic regulation of cell fate choice. Development 136: 3531–3542

Schuettengruber B, Cavalli G (2013) Polycomb domain formation depends on short and long distance regulatory cues. PLoS ONE 8: e56531

Schütze K, Harter K, Chaban C (2009) Bimolecular fluorescence complementation (BiFC) to study protein-protein interactions in living plant cells. Methods Mol Biol 479: 189–202

Schwartz YB, Pirrotta V (2008) Polycomb complexes and epigenetic states. Curr Opin Cell Biol 20: 266–273

Shen L, Thong Z, Gong X, Shen Q, Gan Y, Yu H (2014) The putative PRC1 RING-finger protein AtRING1A regulates flowering through repressing MADS AFFECTING FLOWERING genes in Arabidopsis. Development 141: 1303–1312

Simonini S, Kater MM (2014) Class I BASIC PENTACYSTEINE factors regulate HOMEOBOX genes involved in meristem size maintenance. J Exp Bot 65: 1455–1465

Simonini S, Roig-Villanova I, Gregis V, Colombo B, Colombo L, Kater MM (2012) Basic pentacysteine proteins mediate MADS domain complex binding to the DNA for tissue-specific expression of target genes in Arabidopsis. Plant Cell 24: 4163–4172

Wang L, Jahren N, Miller EL, Ketel CS, Mallin DR, Simon JA (2010) Comparative analysis of chromatin binding by Sex Comb on Midleg (SCM) and other polycomb group repressors at a Drosophila Hox gene. Mol Cell Biol 30: 2584–2593

Wanke D, Hohenstatt ML, Dynowski M, Bloss U, Hecker A, Elgass K, Hummel S, Hahn A, Caesar K, Schleifenbaum F, et al (2011) Alanine zipper-like coiled-coil domains are necessary for homotypic dimerization of plant GAGA-factors in the nucleus and nucleolus. PLoS ONE 6: e16070

Wenke K, Wanke D, Kilian J, Berendzen K, Harter K, Piechulla B (2012) Volatiles of two growth-inhibiting rhizobacteria commonly engage AtWRKY18 function. Plant J 70: 445–459

Winter CM, Austin RS, Blanvillain-Baufumé S, Reback MA, Monniaux M, Wu MF, Sang Y, Yamaguchi A, Yamaguchi N, Parker JE, et al (2011) LEAFY target genes reveal floral regulatory logic, cis motifs, and a link to biotic stimulus response. Dev Cell 20: 430–443

Xu L, Shen WH (2008) Polycomb silencing of KNOX genes confines shoot stem cell niches in Arabidopsis. Curr Biol 18: 1966–1971

Yamamoto YY, Yoshitsugu T, Sakurai T, Seki M, Shinozaki K, Obokata J (2009) Heterogeneity of Arabidopsis core promoters revealed by high-density TSS analysis. Plant J 60: 350–362

Yang C, Bratzel F, Hohmann N, Koch M, Turck F, Calonje M (2013) VAL- and AtBMI1-mediated H2Aub initiate the switch from embryonic to post-germinative growth in Arabidopsis. Curr Biol 23: 1324–1329

Zhang X, Germann S, Blus BJ, Khorasanizadeh S, Gaudin V, Jacobsen SE (2007) The Arabidopsis LHP1 protein colocalizes with histone H3 Lys27 trimethylation. Nat Struct Mol Biol 14: 869–871